NIST Technical Note
NIST TN 2333

Test Results Prepared for DuPont Explosion Hazard Lab: Burning Velocity Tests of Halocarbons in Air

Gregory T. Linteris

This publication is available free of charge from:
https://doi.org/10.6028/NIST.TN.2333

NIST NATIONAL INSTITUTE OF STANDARDS AND TECHNOLOGY
U.S. DEPARTMENT OF COMMERCE

NIST Technical Note
NIST TN 2333

Test Results Prepared for DuPont Explosion Hazard Lab: Burning Velocity Tests of Halocarbons in Air

Gregory T. Linteris
Building Energy and Environment Division
Engineering Laboratory

This publication is available free of charge from:
https://doi.org/10.6028/NIST.TN.2333

September 2025

U.S. Department of Commerce
Howard Lutnick, Secretary

National Institute of Standards and Technology
Craig Burkhardt, Acting Under Secretary of Commerce for Standards and Technology and Acting NIST Director

NIST TN 2333
September 2025

Certain equipment, instruments, software, or materials, commercial or non-commercial, are identified in this paper in order to specify the experimental procedure adequately. Such identification does not imply recommendation or endorsement of any product or service by NIST, nor does it imply that the materials or equipment identified are necessarily the best available for the purpose.

NIST Technical Series Policies
Copyright, Use, and Licensing Statements
NIST Technical Series Publication Identifier Syntax

Publication History
Approved by the NIST Editorial Review Board on 2025-03-06

How to Cite this NIST Technical Series Publication
Linteris G (2025) Test Results Prepared for DuPont Explosion Hazard Lab: Burning Velocity Tests of Halocarbons in Air. (National Institute of Standards and Technology, Gaithersburg, MD), NIST Technical Note (TN) NIST TN 2333. https://doi.org/10.6028/NIST.TN.2333

Author ORCID iDs
Gregory T. Linteris: 0000-0001-7232-5742

Contact Information
linteris@nist.gov

Abstract

The laminar burning velocities of six compounds B1, B2, B3, B4, C1, and C2 are desired. Two methods were attempted for the measurements. In the first, a Mache-Hebra nozzle burner produces a premixed, conical, Bunsen-type flame, from which the average burning velocity is determined from the quotient of the total flow and the Schlieren image area. In the second method, based on the work of Powling and Egerton, a flat flame is stabilized between a honeycomb matrix and a wire mesh screen, and the average burning velocity is determined from the visible flame diameter and the total flow.

The burning velocities of C1 and C2 were obtained directly from measurements in the nozzle burner. The compound C1 has a peak burning velocity of (29.3 $\pm$ 0.9) cm/s in dry air (~5 % R.H.) at a fuel – air equivalence ratio ϕ between 1.0 and 1.2, and C2 has a peak value of (73.9 $\pm$ 5.1) cm/s at ϕ = 1.2.

None of the burning velocities of the B compounds were found to be measurable directly in either apparatus. By adding extra oxygen or methane, however, flames could be stabilized, and extrapolations allowed an assessment of the burning velocities under the desired conditions. Tests were performed with dry air for all the agents, and with moist air (50 % R.H.) for B3 and B4.

The compound B2 was estimated to have a peak burning velocity less than 5 cm/s. The compounds B1, B3, and B4 with dry air were estimated to have peak burning velocities of (11.8 $\pm$ 1.5, 7.8 $\pm$ 1.3, and 7.2 $\pm$ 1.6) cm/s respectively. With moist air, B3 and B4 have estimated peak values of (8.8 $\pm$ 0.8) cm/s and (7.3 $\pm$ 1.2) cm/s.

Most of the extrapolated values come from the nozzle burner measurements. Because of the large degree of preheating of the inlet air (often over 200 °C), the Powling burner was found to produce cellular, rather than flat, laminar flames for most of the conditions of interest, and further work is required to use this technique for flame speed measurements. For conditions under which data were obtainable in both devices, the results are consistent.

Keywords

Burning velocity; flame speed; humidity effect on flame speed; hydrofluorocarbons; hydrofluorochlorocarbons; nozzle burner.

Table of Contents

List of Tables

List of Figures

Preface

This work was carried out at NIST in 1999 under sponsorship from the Dupont Explosion Hazards Laboratory and produced the present report of test results. Because NIST was testing materials related to proprietary compounds and manufacturing techniques, there was a non-disclosure agreement that prevented publication of any of the results for three years. That time has passed and the results are of value to the research community, particularly with regard to the flammability of HFC refrigerants, so the report is being published herein. The following table provides the key to the materials discussed in the body of the report.

Sample Key:

Code	Sample
A1	Selected mix of CH4/air/HFC-125 with documented burning velocity
B1	Trans-1,2-dichloroethylene (DCE)
B2	Perfluorobutylethylene (PFBE)
B3	77/23 wt. (89.5/10.5 mol) DCE/PFBE
B4	60/40 wt. (79.2/20.8 mol) DCE/PFBE
C1	1,1-difluoroethane (HFC-152a)
C2	Vinyl Fluoride

Acknowledgments

The author is grateful to Mrs. Michelle Donnelly, Dr. William Grosshandler, and Dr. Wing Tsang for helpful conversations throughout this research. The work was support through funding from the Dupont Explosion Hazards Laboratory, Project Manager: James Johnson.

1. Introduction

The present work was undertaken to provide the burning velocity as a function of the fuel-air equivalence ratio (ϕ) for six compounds in air, designated B1, B2, B3, B4, C1, and C2. The first two are pure liquids, the second two are blended liquids, and the last two are gases at room temperature. The expected range of burning velocity was 5 cm/s to 55 cm/s based on estimations and calculations.

Two separate burners were used. The first is a Mache-Hebra nozzle burner, which had been used extensively at NIST during the mid-1990s to determine the burning velocity of hydrocarbon – air flames inhibited by halocarbons and other agents. This burner, described in detail below, is well characterized, and has been found suitable for burning velocities in the range of 7 cm/s to 60 cm/s. This range of operation might be expected to be inclusive of nearly all of the desired burning velocities; however, it is also known that not all reaction mixtures provide stable flames over the entire range of operation (unstable flames lift off from the burner). For example, the burning velocity of methane - air flames with the added hydrofluorocarbons $C_2H_2F_4$, or C_2HF_5 can be determined down to about 7 cm/s; whereas for pure methane-air flames varied over a range of stoichiometry, the minimum burning velocity obtainable is only 20 cm/s on the lean side and 15 cm/s on the rich side. It is generally not known a priori if flames of a particular mixture will be stable on the nozzle burner under the required conditions.

The second approach used is that of Powling [1]. The burner, described below, has been used to measure the burning velocity of lean limit flames in the range of 5 cm/s to 15 cm/s [2, 3]. For these conditions, the Powling burner produces flat flames which are separated from any surface by about 1 cm, so conduction losses are low. Unfortunately, the flames are not adiabatic, since the screen above the burner exit, necessary to stabilize the very slow-burning flames, is heated from the post-combustion gases and radiates back to the burner surface. Gases exiting the burner surface can have preheats of up to several hundred degrees C.

Several approaches can be used to extend the range of both burners. For example, mixtures that are too weak to produce a stable flame can be enriched by adding a more reactive species such as methane, or the reaction temperature can be increased by adding more oxygen or preheating. The burning velocities under the desired conditions, where the present burners may be inoperable, can then be obtained by extrapolation from the measured conditions. This report describes the experimental methods, presents the results of measurements, and discusses the utility of the two burners and the interpretation of data obtained using them. Recommendations for future approaches are also provided.

2. Experimental Methods

The nozzle burner is based on the design of Mache and Hebra [4], with some modifications. The experimental system has been described in detail previously [5, 6]. The burner consists of a quartz tube 27 cm long with an area contraction ratio of 4.7 (over a 3 cm length) and a final nozzle diameter of (1.02 ± 0.005) cm, which is placed in a square acrylic chimney 10 cm wide and 86 cm tall. There is provision for co-flowing air or nitrogen gas (for the present data, the co-flow gas is air, and the flow rate is selected to provide the most stable flame). A schlieren imaging system [7] provides the flame area from which the average burning velocity of these Bunsen-type flames is determined using the total area method [8]. An optical system (a white-light source with a vertical slit at its exit, lenses, a vertical band, and filters) generates the schlieren image of the flame for capture by a 776 x 512 pixel Charged Injection Device (CID) array (Cidtec CID3710D). The image is digitized by a 640 pixel x 480 pixel frame-grabber board (Data Translation 3155) in a Pentium-II computer. The images are acquired and written to disk using the free University of Texas Health Science Center of San Antonio (UTHSCSA) ImageTool program [9]. The flame area is determined (assuming axial symmetry) using custom image-processing software, and the burning velocity is calculated by dividing the volumetric flow rate (corrected to 10133 Pa and 298 K) by the flame area.

For the present data, the visible flame height is maintained at a constant value of 1.3 cm to provide a similar rate of heat loss to the burner, while the desired equivalence ratio is preserved. The experimental technique is similar to that used extensively by Van Wonterghem and Van Tiggelen [7]. The present burner, however, is larger, providing less curvature and strain; the flame holder is not water-cooled and the material (quartz) has a much lower thermal conductivity, reducing heat losses to the burner; the ratio of the flame height to the burner diameter is smaller so that there is less curvature, strain, and buoyancy-driven flow; and the burner is enclosed in a chimney with provision for any co-flow gas. The mass flow controllers provide additional flexibility in the operation of the burner. In these experiments, the low rate of heat loss to the burner, the low strain rate, and the low curvature facilitate comparisons of the burning velocity with those of an idealized one-dimensional adiabatic flame. Although the burning velocity in Bunsen-type flames is known to vary at the tip and base of the flame and is influenced by curvature and stretch [8], these effects are most important over a small portion of the flame.

The burner produces straight-sided schlieren and visible images which are very closely parallel. Gas flows are measured with digitally-controlled mass flow controllers (Sierra Model 860) with a quoted repeatability of 0.2 % and accuracy of 1 % of full-scale flow which have been calibrated with bubble (Gillian Gilibrator) and dry (American Meter Co. DTM-200A) flow meters so that their accuracy is 1 % of indicated flow. House compressed air (filtered and dried) is used after it has been additionally cleaned by passing it through an 0.01 μm filter, a carbon filter, and a desiccant bed to remove small aerosols, organic vapors, and water vapor. Methane (Matheson UHP); oxygen (MG Industries, H_2O < 50 ppm, total hydrocarbons < 5 ppm) and nitrogen (boil-off from liquid N_2) were also used.

For addition of liquid fuels, two computer-controlled stepper-motor driven syringe pumps (Yale Apparatus model YA-12) located in a chemical fume hood feed the fuel at room temperature (21.5 °C) through a series of check valves. The system allows accurate delivery of small volumes of liquid nearly continuously (one pump feeds fluid while the other withdraws fluid from the supply reservoir, and there is a slight discontinuity in the flow rate when the syringe pumps change direction). The liquid flows to an evaporator which consists of a 2.36 cm I.D. and 30.5 cm long stainless-steel tube packed with 3 mm diameter glass beads. Resistive heating wires and insulation surround the tube, and a single temperature controller maintains the temperature at the point of liquid injection to 60 °C. Fuel enters through a 3.2 mm O.D. stainless steel tube, and a carrier gas (the air stream) carries the liquid through the packed bed where it evaporates. The peak temperature downstream of the fuel injection reaches up to 150 °C during some tests. Precision glass/Teflon syringes (Hamilton Gas-tight, (2.5, 5.0, 10, 25, and 50) cm^3) provide gas-tight seals and relatively smooth operation of the liquid feed system. The smallest syringe possible is selected from the collection to provide the fastest piston speed yet a long enough test time before syringe pump direction reversal (during which the data collection is halted).

For water vapor addition, a cooling bath temperature controller (Neslab Crytrol) maintains the temperature of a stirred water bath vessel (23 L) to (11.1 ± 0.1) °C. Two saturators in series, each consisting of a glass tube 40 cm long and 10 cm in diameter with a porous glass frit at the base, inject the carrier gas bubbles to their volume of de-ionized water. The system is calibrated for the degree of saturation by measuring the water vapor content of the output air (Extech Instr.). Gas flow rates through the system range from 1 L/min to 20 L/min, and water vapor is typically added at a mole fraction of 1.5 %, which corresponds to a relative humidity of about 50 %.

A flat-flame burner modeled after that of Powling [1] was constructed with some modifications. A schematic of the burner is shown in Fig. 1. A flat flame is stabilized midway between the upper rim of the inner Pyrex tube and the stabilizing screen. A flow straightener is located about 8 mm below the rim of the Pyrex. In their design, this straightener consists of a 22 mm thick, 6 cm diameter honeycomb matrix, made by winding together alternating strips of flat and corrugated cupro-nickel alloy ribbon. This metal is not suitable for the present studies since B1 is reactive with copper-containing alloys. Instead, an Al_2O_3 ceramic honeycomb matrix, also 22 mm thick and 6.0 cm in diameter was used. A 5 cm thick bed of Pyrex beads (3 mm diameter) sits below this matrix, followed by another flow straightener of the same size and type. Two fine thermocouple wires (Omega type K, 300 μm bead diameter) pass through these layers, and the beads are situated just below the surface of the ceramic burner in one of the gas-flow channels. In our design, in order to overcome possible etching of the glass by hydrogen halides, the top 8 cm of the outer Pyrex tube is replaceable, and a water-cooled acrylic chimney can also be used. Either 30 mesh or 40 mesh stainless steel screens were used as the flow stabilizer at the top. The thermocouple voltage outputs were measured with a calibrated analog to digital

converter board in a personal computer. Gas flows and water vapor addition were controlled as described above. The flame size and appearance were captured by a color CCD camera and an SVHS video recorder saved the images to video tape when desired.

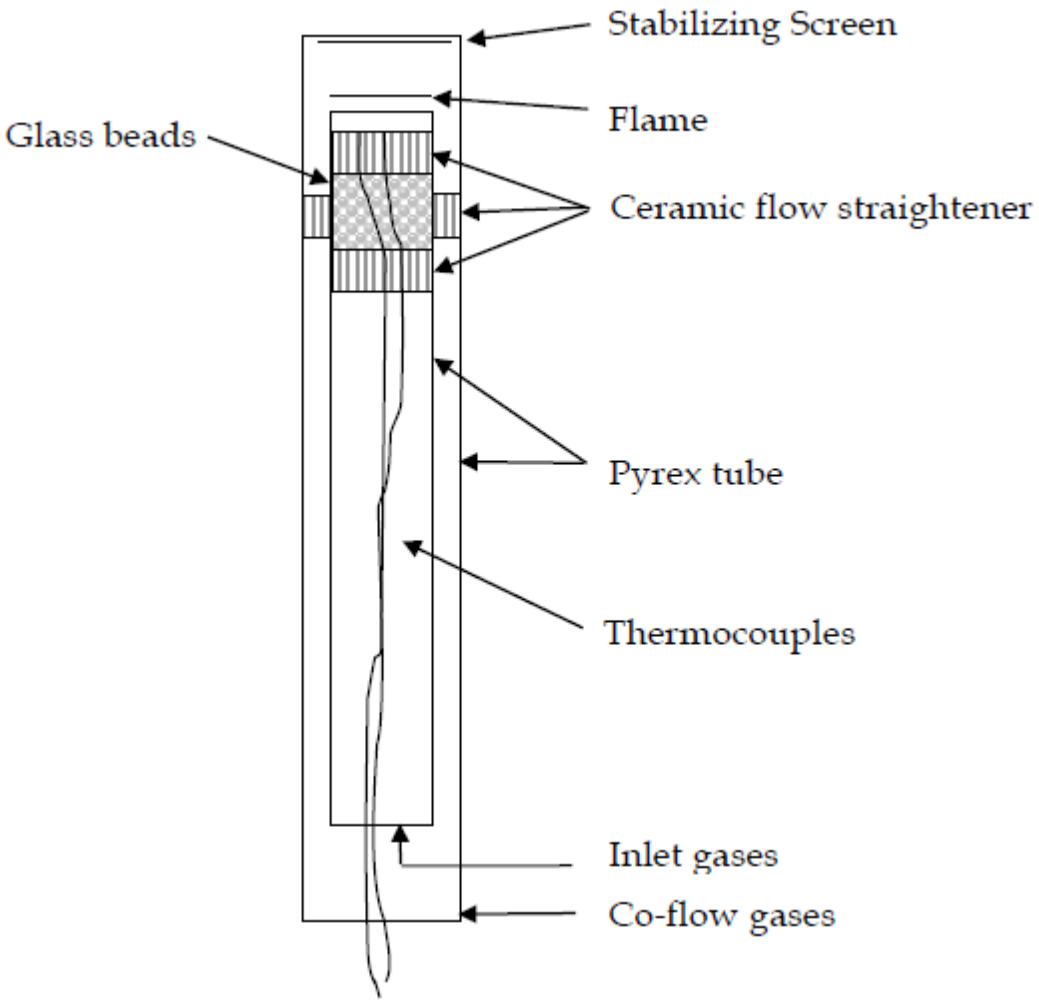

Fig. 1. Schematic of Powling burner.

3. Results

The experimental results are presented for each compound tested, with separate discussions for the two burners used. The Powling burner was generally found to be unsuitable for many of the pure fuels. The agent B1 has wrinkled flames rather than flat, laminar flames, and the agent B3 caused too much heating of the burner, and again, subsequently wrinkled flames. Fig. 2 shows a B3 – moist air flame in the Powling burner in which the air is preheated by the burner surface to 185 °C; the flame is clearly not flat or laminar. We could not light pure B2 in the Powling burner. By adding methane, we could stabilize flames with 1 % to 1.3 % CH_4, but these had burning velocities too low to measure (<3 cm/s). We could not light and stabilize flames of pure B4 and dry air (tested only at stoichiometric conditions), and even with added methane, the flames were difficult to stabilize. Typically, most of the initial tests were done at ϕ=1.0; trying the Powling burner with pure B4 at ϕ=1.2 might prove more effective.

To obtain data with B1, B2, B3, and B4, we operated the nozzle burner with added methane, or with oxygen enrichment, as described below, and extrapolate to the conditions of the pure fuels. The burning velocities of agents C1 and C2 were tested successfully in the nozzle burner over a range of ϕ.

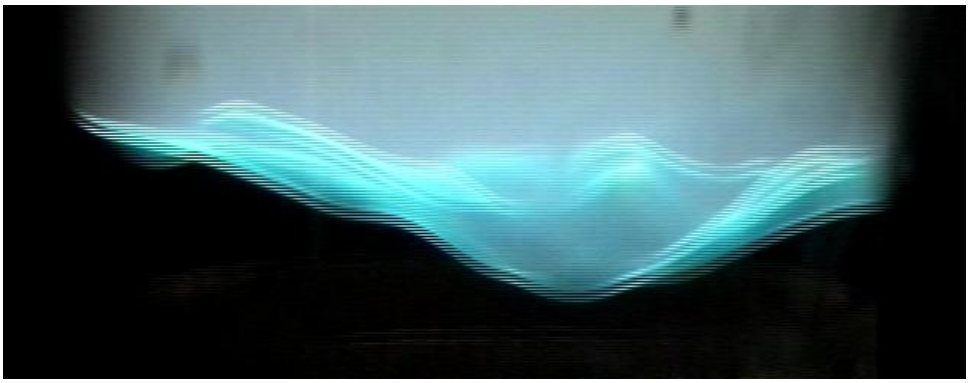

Fig. 2. Image of B3 flame in Powling burner with moist air and a preheat of 185℃.

3.1. Agent B1

3.1.1. Nozzle Burner

Pure flames of B1 would burn in the nozzle burner, but unfortunately, the flame shape was not amenable to accurate flame speed measurements. The flame was lifted, the position above the burner oscillated, and the flame shape was curved, indicating a strong variation of the burning velocity over the flame surface. In order to determine the approximate burning velocity of pure flames of B1 with air, we conducted experiments in which flames of methane-air at the desired stoichiometry were first stabilized, and then the methane was gradually replaced by B1. The parameter X is used to determine the volume fraction of methane and B1 in the fuel stream:

X=0 refers to pure methane, X=0.5 is half methane and half B1, and X=1 refers to pure B1. For all cases, the stoichiometry is maintained at a constant desired value, withϕ =1.0 corresponding to reaction to the most stable products: H_2O, CO_2, HBr, HF, and HCl which are formed preferentially over H_2O.

Fig. 3 shows the burning velocity of B1 – air flames for ϕ =1.0, 1.1, and 1.2. Flames with 80 % B1 and 20% CH_4 as the fuel could be stabilized for □ =1.0 and 1.1, and 90 % B1 and 10 % CH_4 with ϕ = 1.2. The values of the burning velocity extrapolated to X=1.0 are (8.3, 10.5, and 11.8) cm/s for ϕ = 1.2, 1.1, and 1.0 respectively. Note that these tests were performed with dried house compressed air (further filtered and dried as described above) which has a relative humidity of about 5%.

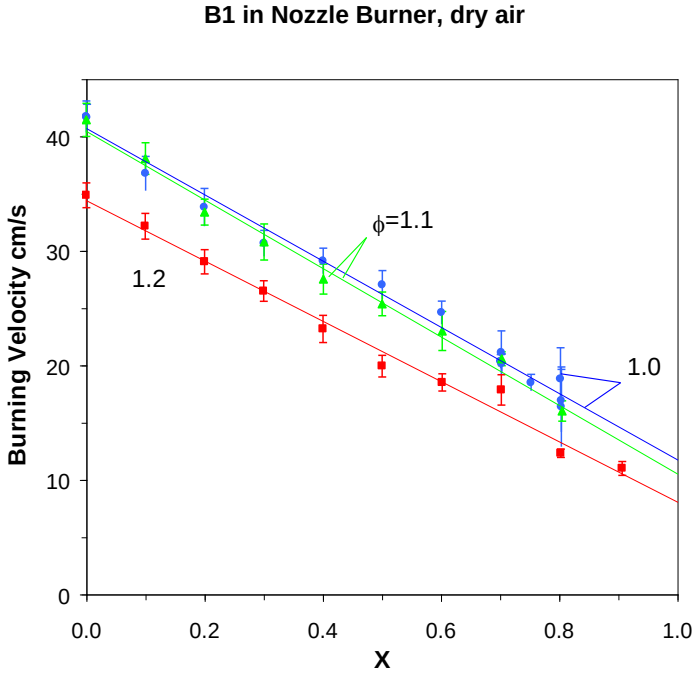

Fig. 3. Measured burning velocity of B1 - methane –air (dry) mixtures as a function of X, the B1 mole fraction in the fuel, for ϕ = 1.0, 1.1, and 1.2. The lines are linear least-squares curve fits to the data.

3.1.2. Powling Burner

Flames of B1 – air in the Powling burner, even with the dry air, started off laminar, but as the stabilizing screen heated the burner surface by radiation, the flames quickly (in less than 20 seconds) became cellular and wrinkled as in Fig. 2. Accurate flame speed measurement by the method of Powling are not possible under these conditions. Burner exit velocities of 16 cm/s failed to prevent the flame from approaching the burner surface; however, the gas inlet temperatures quickly rose above 100 °C, so that measurements at inlet temperatures near room temperature (about 21 °C) were not possible.

3.2. Agent B2

3.2.1. Nozzle Burner

Section reference Flames of pure B2 – air with dry air would not stabilize in the nozzle burner. Using the technique described above, replacing methane with B2 as the fuel, we obtained the data shown in Fig. 4, in which the burning velocity is plotted as a function of X. Both a linear curve fit and a third-order polynomial fit are shown. The extrapolations indicate that pure B2 with dry air will not burn (a flame speed of 5 cm/s is typically considered to be the flammability limit). It is interesting to note the apparent change in slope shown in the figure. Above X=0.6, replacement of CH_4 by B2 decreases the burning velocity much faster than below this value; analysis shows that at X=0.6, the halogen to hydrogen ratio in the reactant stream just goes above 1.0. Previous results [5] have shown that the rate of reaction is greatly reduced at halogen to hydrogen ratios above unity for hydrocarbon – air flames with halogens.

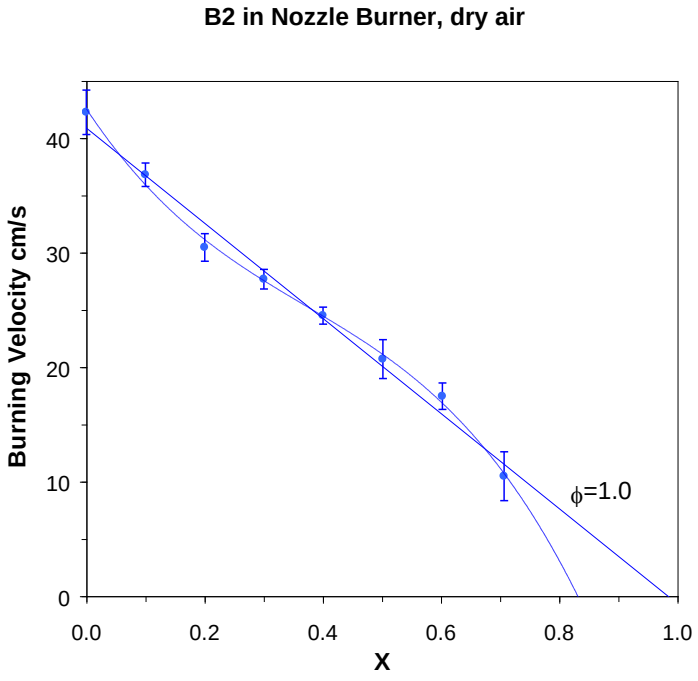

Fig. 4. Measured burning velocity of B2 - methane –air (dry) mixtures for stoichiometric conditions with dry air as a function of X, the B2 mole fraction in the fuel. The lines are linear, and third-order polynomial least-squares curve fits to the data.

3.2.2. Powling Burner

We could not ignite flames of pure B2 – dry air in the Powling burner. To obtain stable flames, we added methane (at 1 % to 1.3 % of the total flow) to flames with ϕ=1.1. Under these conditions, stable flames were achieved with gas inlet temperatures of 125 K to 150 K, and

burner gas exit velocities of 2.1 cm/s to 2.3 cm/s. Even at ϕ=1.2 (where the burning rate should be higher), with 1 % CH_4 and 216 °C preheat, a burner gas exit velocity of only 6 cm/s matched the flame propagation rate. Hence, the burning velocity of pure B2 with no preheat is clearly less than 5 cm/s.

3.3. Agent B2

3.3.1. Nozzle Burner

Flames of B4 were tested in the nozzle burner in two separate ways: varying the B4 - methane ratio or varying the oxygen mole fraction in the oxidizer stream. Both of these approaches permit extrapolation back to combustion of B4 with ambient air. In the first sequence of tests, methane was replaced in increasing fraction by B4 as described above for B1 and B2. The burning velocity of B4 – methane blends as a function of X are shown in Fig. 5 for tests with dry air and values of ϕ = 1.0, 1.1 and 1.2. The velocities for pure B4 and dry air are estimated from extrapolation to be ≈0 cm/s, 3.7 cm/s, and 7.2 cm/s for each value of ϕ, respectively. These tests were performed with dry shop air (which typically has a relative humidity of 4 % or 5%). In order to determine the effect of added water vapor, we performed additional tests in which known quantities of water vapor were added.

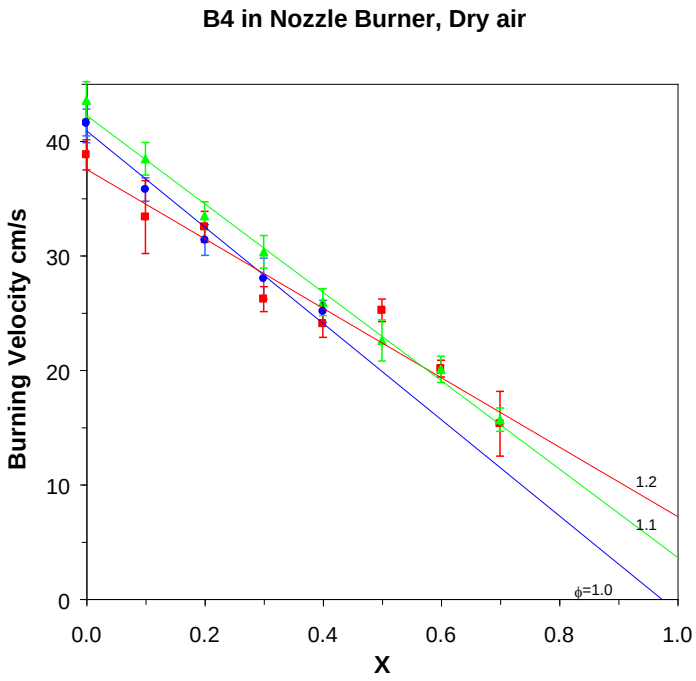

Fig. 5. Measured burning velocity of B4 - methane –air (dry) mixtures as a function of X, the B4 mole fraction in the fuel, for ϕ = 1.0, 1.1, and 1.2. The lines are linear least-squares curve fits to the data.

Figures 6, 7, and 8 show the effect of added water vapor on the burning velocities of B4 – air flames at ϕ=1.0, 1.1, and 1.2. Water vapor is added to the air stream at values corresponding to approximately 50 % relative humidity at room temperature, or a mole fraction of about 1.5 %. The added water vapor tends to lower the burning velocity of pure CH_4 – air flames (X=0) since the system in not hydrogen limited, and the added H_2O acts as a diluent to lower the temperature. For systems with increasing B4 content, however, H atoms, necessary for the chain-branching radical reactions which provide the high overall reaction rates, quickly react with the halogen atom, and are less or un-available for further reaction. Hence, at high values of X, the added water vapor typically increases the burning velocity, so that stoichiometric and slightly rich (ϕ=1.1) flames of pure B4 and moist air have significantly higher estimated burning velocities than for dry conditions (2.9 cm/s vs 0 cm/s for ϕ=1.0, and 5.6 cm/s vs. 3.7 cm/s for ϕ=1.1). The importance of water vapor appears to decrease as ϕ increases, and for ϕ=1.2, the moist and dry flames have the same extrapolated burning velocity at X=1.0 (7.2 cm/s). It should be emphasized that while these trends are consistent with other results [5, 10, 11], the burning velocities for pure B4 –air flames (X=1.0) are from extrapolations and the exact functional relationship of the curves in Fig 4 are not known. Insight could be determined through further tests and detailed numerical calculations.

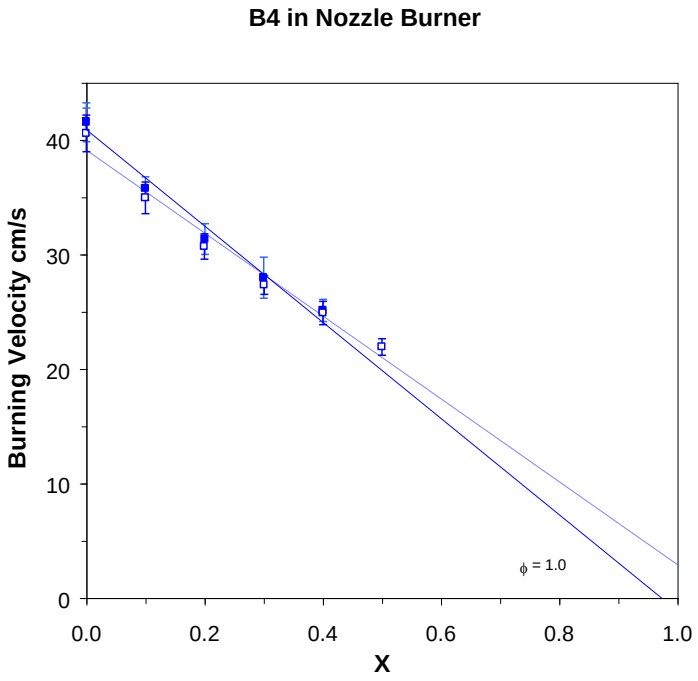

Fig. 6. Measured burning velocity of B4- methane –air mixtures for ϕ = 1.0 as a function of X, the B4 mole fraction in the fuel. The closed symbols and solid lines are for dry conditions, and open symbols and dotted lines are with an H_2O mole fraction of 1.5 % in the mixture. The lines are linear least-squares curve fits to the data.

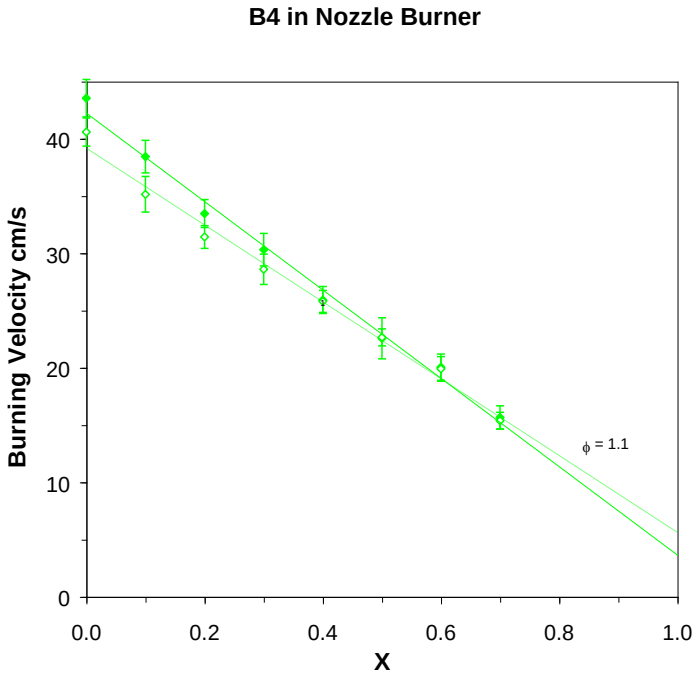

Fig. 7. Measured burning velocity of B4 - methane –air mixtures for ϕ = 1.1 as a function of X, the B4 mole fraction in the fuel. The closed symbols and solid lines are for dry conditions, and open symbols and dotted lines are with an H_2O mole fraction of 1.5 % in the mixture. The lines are linear least-squares curve fits to the data.

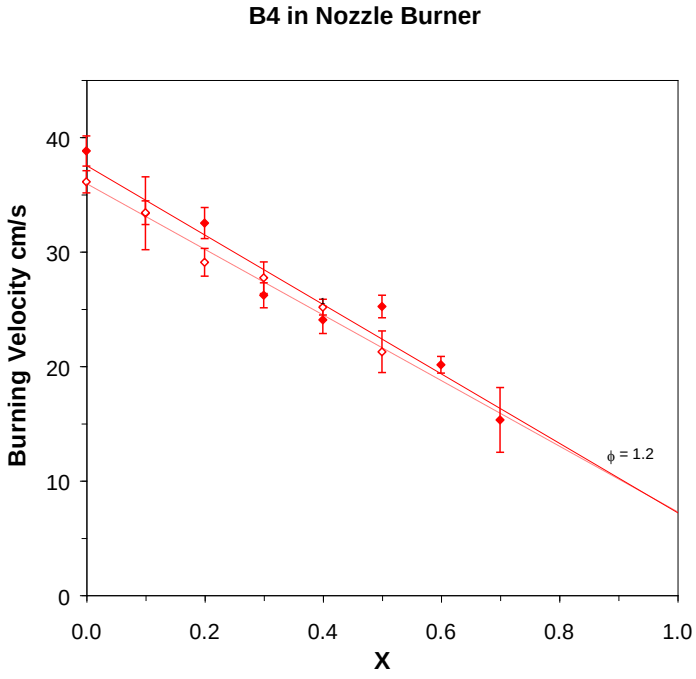

Fig. 8. Measured burning velocity of B4 - methane –air mixtures for ϕ = 1.2 as a function of X, the B4 mole fraction in the fuel. The closed symbols and solid lines are for dry conditions, and open symbols and dotted lines are with an H_2O mole fraction of 1.5 % in the mixture. The lines are linear least-squares curve fits to the data.

In order to provide another avenue for examining the burning velocity of B4 – air flames, we tested pure B4 in the nozzle burner with an oxidizer of varying oxygen mole fraction $X_{O_2,ox}$. Since our sources of nitrogen (boil-off) and oxygen (<50 ppm H_2O) are very dry, we ran these tests with added water vapor to allow comparisons with the tests in which the methane – B4 ratio was varied, for ϕ=1.0 with moist air (Fig. 6) above. Figure 9 shows the measured burning velocity of pure B4 – oxidizer flames in which the value of $X_{O_2,ox}$ is varied. The extrapolated value for 21 % oxygen is about 4.3 cm/s which compares to the extrapolated value from Fig. 6 of 2.9 cm/s. Given the uncertainty in both the measurements and the extrapolations, these results are consistent, and B4 at ϕ=1.0 has a very low burning velocity—if measurable.

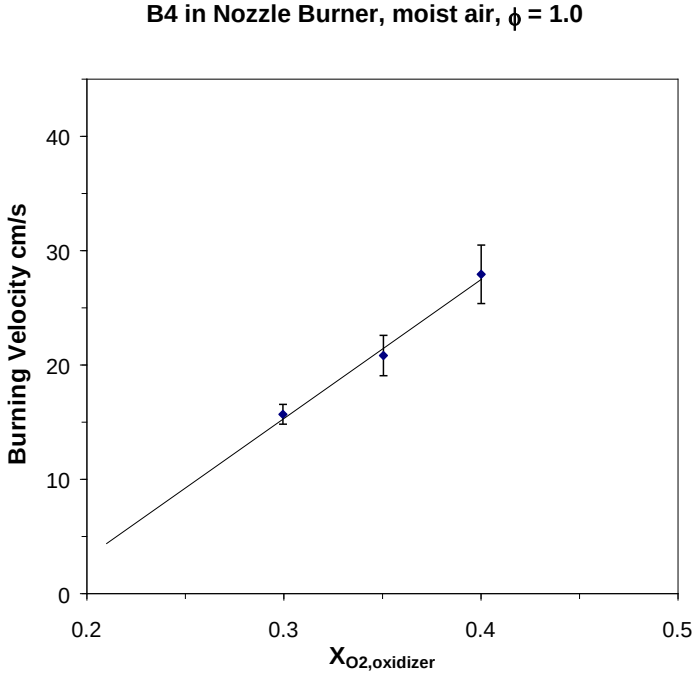

Fig. 9. Measured burning velocity of B4 – oxidizer mixtures for ϕ = 1.0 as a function of the oxygen mole fraction in the oxidizer $X_{O_2,ox}$ with added water vapor at 1.5 % volume fraction. The lines are linear least-squares curve fits to the data.

3.3.2. Powling Burner

We could not light B4 in the Powling burner without added methane. With added methane, we obtained the data in Fig. 10 in which the gas exit velocity from the burner is plotted as a

function of added methane for stoichiometric flames (here, ϕ is based on the oxygen requirements of B4 only). These data clearly represent upper limits on the burning velocity of pure B4 with dry air for the following reasons. First, the flame area was not measured but appeared to be larger than the burner exit area. Use of the actual flame area would yield a value of the burning velocity lower than the gas exit velocity. Second, these flames have significant preheat (103 °C to 233 °C). As will be shown below in tests with B3, this much preheat can increase the burning velocity by about a factor of two. Hence, while these tests imply that the burning velocity for dry B4 – air flames with no CH_4 and at ambient temperature would be something less than 6.4 cm/s, measuring the flame size and correcting for the preheat would provide lower values (note that the extrapolated value from B4/methane tests for stoichiometric pure B4 – dry air flames from the nozzle burner imply a burning velocity 0 cm/s).

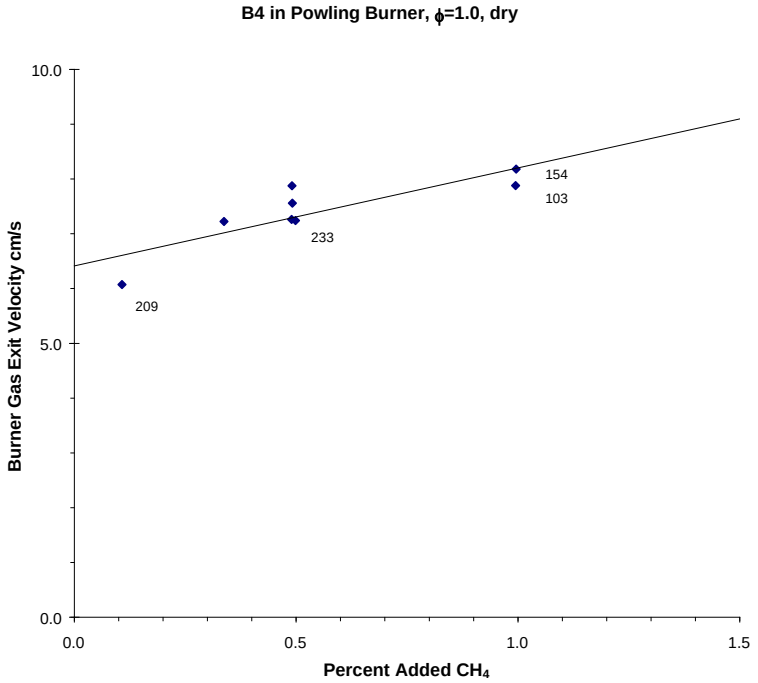

Fig. 10. Gas exit velocity in the Powling burner necessary to stabilize a flame, as a function of the added methane mole fraction for ϕ=1.0 (based only on B4). The inlet temperature (in C) of the gas is noted next to points for which it was available.

3.4. Agent B3

3.4.1. Nozzle Burner

The results of tests of B3 and methane in the nozzle burner are presented in Fig. 11 which shows the burning velocity of B3 – CH_4 blends as a function of X for dry air at ϕ=0.9, 1.0, 1.1, and 1.2. Figures 12, 13, and 14 show the results for each value of ϕ for both moist and dry air

cases, except ϕ=0.9 with moist air for which flames could not be stabilized. Figure 12 for B3 shows that unlike all other cases, the extrapolated value for moist flames at ϕ=1.0 is actually lower than that for dry flames; Figures 13 and 14 show the more usual trend of increasing burning velocity of pure fuel with moist air. Figure 15 shows the data for all moist flames of B3 (ϕ=1.0, 1.1, and 1.2) in the nozzle burner. The richest flames shown, ϕ=1.2, again have the highest extrapolated burning velocity, 8.8 cm/s, slightly higher than the ϕ=1.1 case (7.9 cm/s).

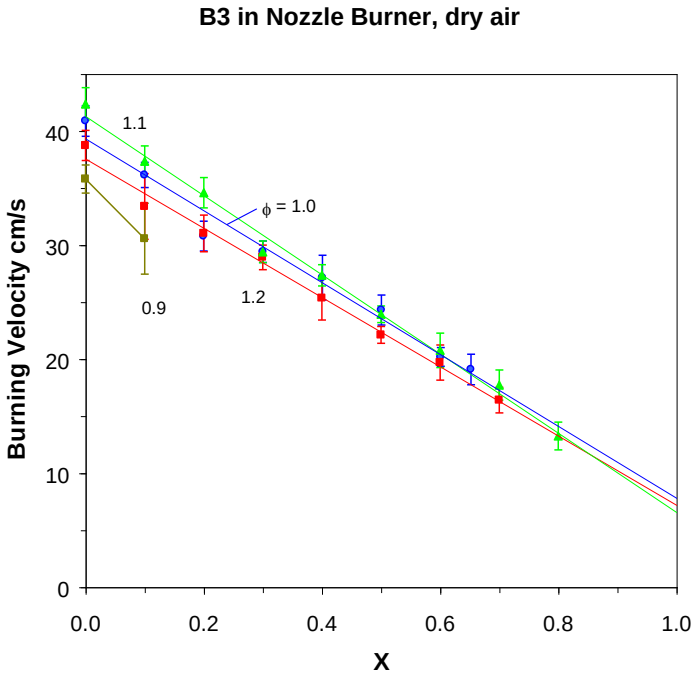

Fig. 11. Measured burning velocity of B3 - methane –air (dry) mixtures as a function of X, the B3 mole fraction in the fuel, for ϕ = 0.9, 1.0, 1.1, and 1.2. The lines are linear least-squares curve fits to the data.

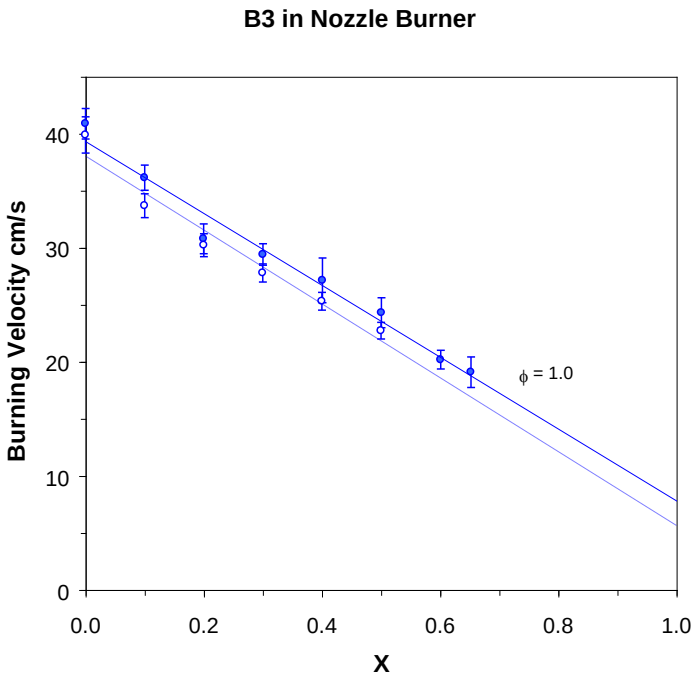

Fig. 12. Measured burning velocity of B3 - methane – air mixtures for ϕ = 1.0 as a function of X, the B3 mole fraction in the fuel. The closed symbols and solid lines are for dry conditions, and open symbols and dotted lines are with an H_2O mole fraction of 1.5 % in the mixture. The lines are linear least-squares curve fits to the data.

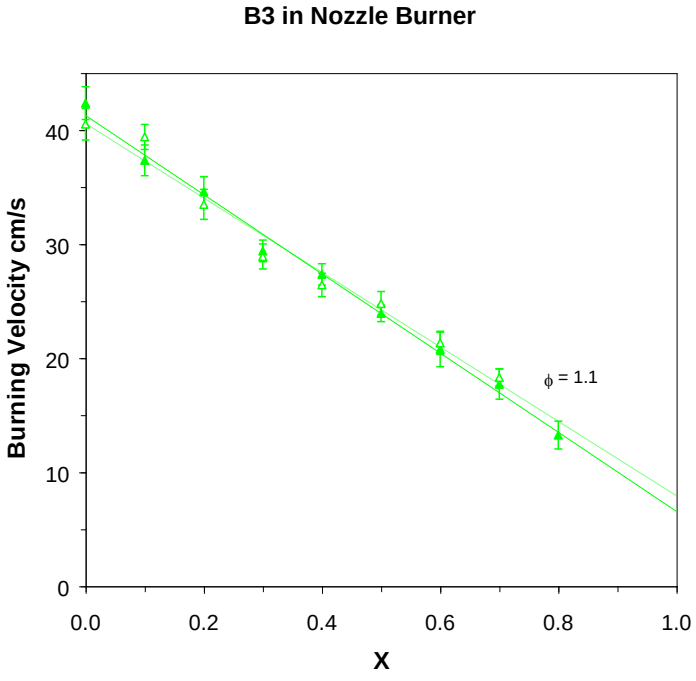

Fig. 13. Measured burning velocity of B3 - methane – air mixtures for ϕ = 1.1 as a function of X, the B3 mole fraction in the fuel. The closed symbols and solid lines are for dry conditions, and open symbols and dotted lines are with an H_2O mole fraction of 1.5 % in the mixture. The lines are linear least-squares curve fits to the data.

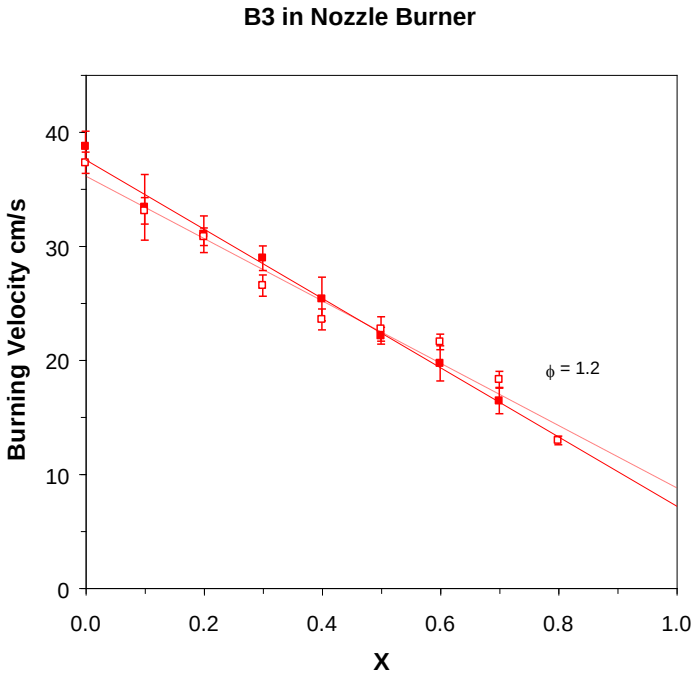

Fig. 14. Measured burning velocity of B3 - methane – air mixtures for ϕ = 1.2 as a function of X, the B3 mole fraction in the fuel. The closed symbols and solid lines are for dry conditions, and open symbols and dotted lines are with an H_2O mole fraction of 1.5 % in the mixture. The lines are linear least-squares curve fits to the data.

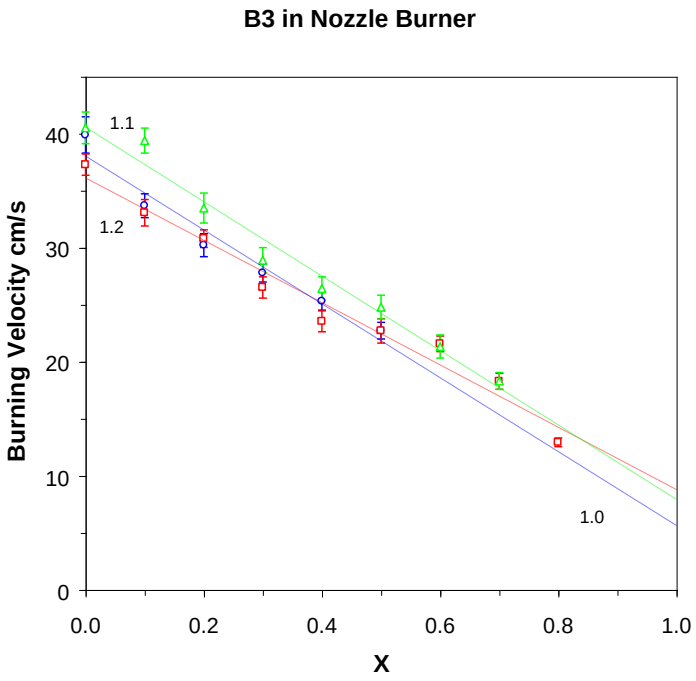

Fig. 15. Measured burning velocity of B3 - methane – air (moist) mixtures as a function of X, the B3 mole fraction in the fuel for ϕ = 1.0, 1.1, and 1.2. The lines are linear least-squares curve fits to the data.

3.4.2. Powling Burner

We could not stabilize *steady* flames of B3 in the Powling burner. The flames heat the stabilizing screen, which radiates back to the ceramic burner surface, heating it. Even with the flame about 2 cm from the burner surface, the temperature of the inlet gases rises above 150 ℃ in less than a minute, increasing the burning velocity, and causing the flame to approach the burner surface. If the experiment were continued at a fixed flow rate of gases from the burner, the burning velocity would become greater than the gas exit velocity, and the flame would settle on the burner surface. In practice, one can increase the flow of gases in real time, attempting to keep the flame approximately midway between the burner and the stabilizing screen. In this approach, the required gas exit velocity from the burner is a function of the inlet temperature. For some flames, for example the dry B4 flames in Fig. 10 above, the flame remained laminar as a pseudo-steady condition was reached. For both B1 and B3, however, a steady condition was not possible since as the flow rate was increased, the flames wrinkled due to instabilities (as shown in Fig. 2).

In order to try to get useful numbers from the burner despite that fact that steady flames were not possible, we collected data in a transient way as described here. The flame was lit with the premixed gas flow velocity preset to a value which approximately balanced the burning velocity. As the flame heated the burner, the inlet temperature increased, thereby increasing the flame speed. The gas flow rate and liquid pumping rates were set, in real time, to a higher

value to again balance the flame position, and the flows and temperatures were recorded. This process continued until the flame became wrinkled. The whole event occurs over a total time of less than 30 s. This technique allows one to obtain data, but because there are many non-steady phenomena occurring with a time constant comparable to the test time, there is significant scatter in the data. For example, the heating of the screen and burner surface as well as other parts of the burner are non-steady, the evaporation of the fuel also has a transient when the flow rate is changed, and the mass flow controllers for the gas flows have a non-zero settling time. Data from a number of tests of B3 and dry air in the Powling burner are shown in Fig. 16. Although the large scatter in the data is evident, the figure shows the strong dependence of the burning rate on the inlet gas preheat—about a factor of two for 200 °C. This result is consistent with the finding of Egerton and Thabet [2] in their studies of near-limit ethylene-air flames. Because of the transient nature of the data, it did not seem warranted to record and analyze the flame areas from the video images which were constantly viewed during the tests; alternatively, the data are presented as the gas exit velocity from the flat burner. If a flat flame were possible, its area would have been within 10 % of the burner exit area. There is too much scatter in the data in Fig. 16 to warrant an extrapolation to an inlet temperature of 21 °C, especially considering that the flame areas were not measured. It is interesting to note that an extrapolated burning velocity from Fig. 16 would yield a value about a factor of two lower than the extrapolated value from the nozzle burner—a result similar to the B4 results described above.

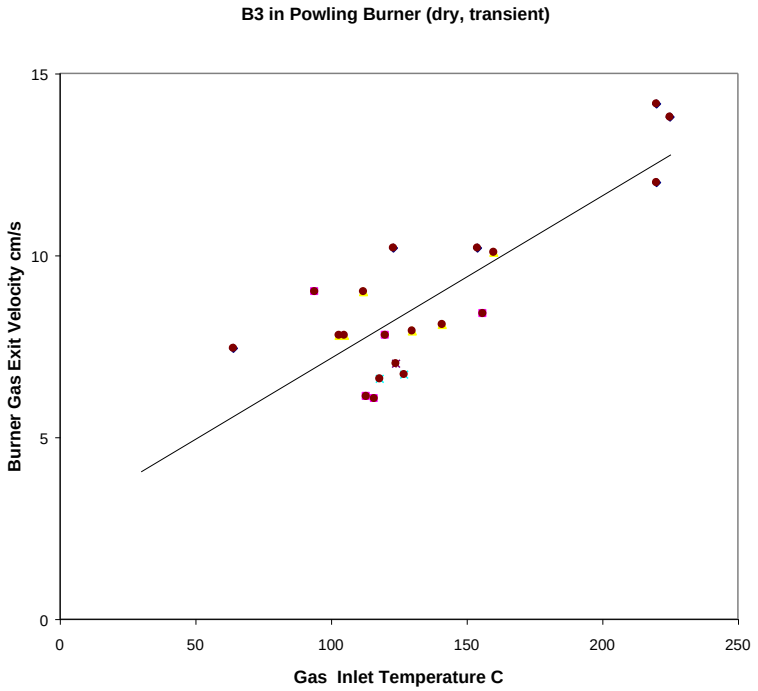

Fig. 16. Transient test results of the measured gas exit velocity in the Powling burner for B3 – air (dry) as a function of the indicated inlet gas temperature.

3.5. Agent C1

3.5.1. Nozzle Burner

The agent C1 was tested in the nozzle burner with dry shop air over a range of ϕ, and the data are presented in Fig. 17. The burning velocity is relatively constant in the range $1.0 \leq \phi \leq 1.2$, and the peak value is 29.3 cm/s. The flames were blue and steady in the range of $0.9 \leq \phi \leq 1.3$, providing nice schlieren images. In richer conditions, $1.3 \leq \phi \leq 1.5$, flames were stabilized, but they were open tipped. At ϕ=1.5, the flame became cellular and unstable on the upper half and had a faint yellow glow above the open tip. There was clear after-burning in the region about 1 cm downstream of the main reaction zone, indicating that the flame was behaving as a partially premixed diffusion flame.

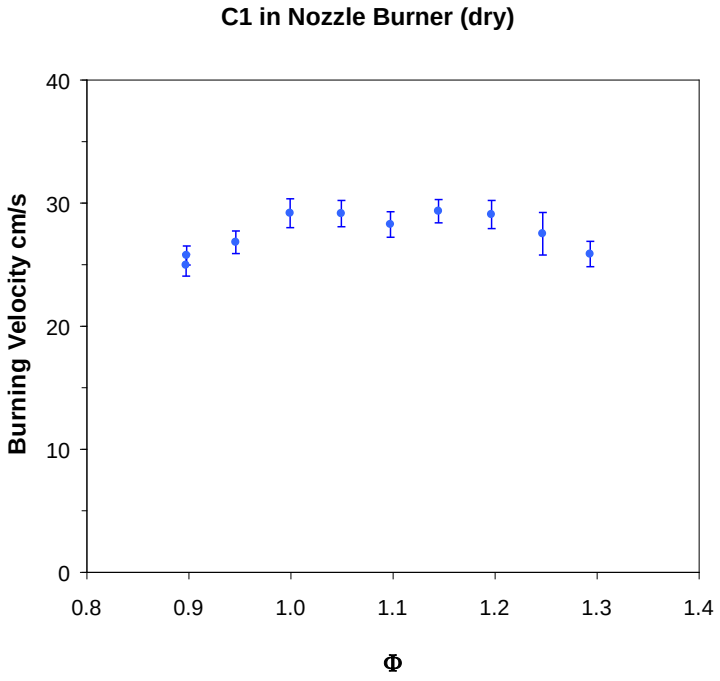

Fig. 17. Measured burning velocity of C1 in nozzle burner as a function of the fuel – air (dry) equivalence ratio ϕ.

3.6. Agent C2

3.6.1. Nozzle Burner

The agent C2 was also tested in the nozzle burner with good results. Figure 18 shows the burning velocity as a function of the fuel air equivalence ratio for $0.7 \leq \phi <= 1.5$. The peak burning velocity occurs at ϕ=1.2, where it is equal to 73.5 cm/s. There was some wrinkling of the flame tip for the higher-speed flames in the present data, and this shows up, to some extent, in the larger uncertainty for those data points. The actual burning velocity for laminar, unwrinkled flames may be slightly less than the given values. The flames were bright blue and very stable.

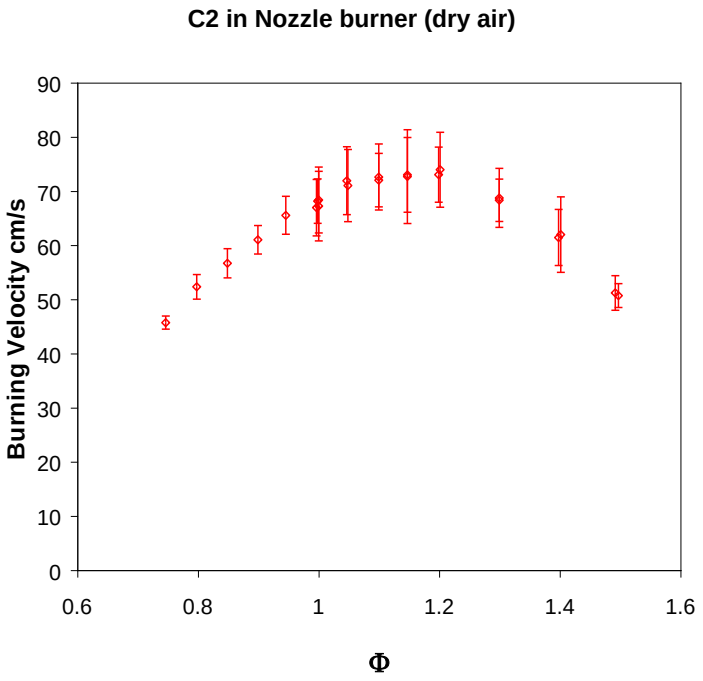

Fig. 18. Measured burning velocity of C2 in nozzle burner as a function of the fuel – air (dry) equivalence ratio ϕ.

4. Discussion

The results of the extrapolations from the measurements in the nozzle burner are presented in Fig. 19 below. The estimated burning velocity of flames of B4, B3, and B1, with dry air (solid lines) are shown for ϕ=1.0, 1.1, and 1.2, as a function of the mole fraction of B1 in each mixture. As the figure indicates, for dry flames at ϕ=1.2, the estimated burning velocity is nearly constant at about 8 cm/s; as ϕ approaches unity, there is a very strong dependence on the amount of B2 in the mixture. With added water vapor (dotted lines), the dependence on B2 content is decreased. For ϕ=1.1 and 1.2, there is a moderate increase in the extrapolated burning velocity with water vapor, and the two curves approach each other; while for ϕ=1.0, the strong dependence on B2 content is reduced, so that the estimated burning velocity of B4 increases with moist air relative to dry, and that for B3 decreases with moist air. It would be of interest to obtain the moist values for B1, and moist and dry values for mixtures with greater B2 content.

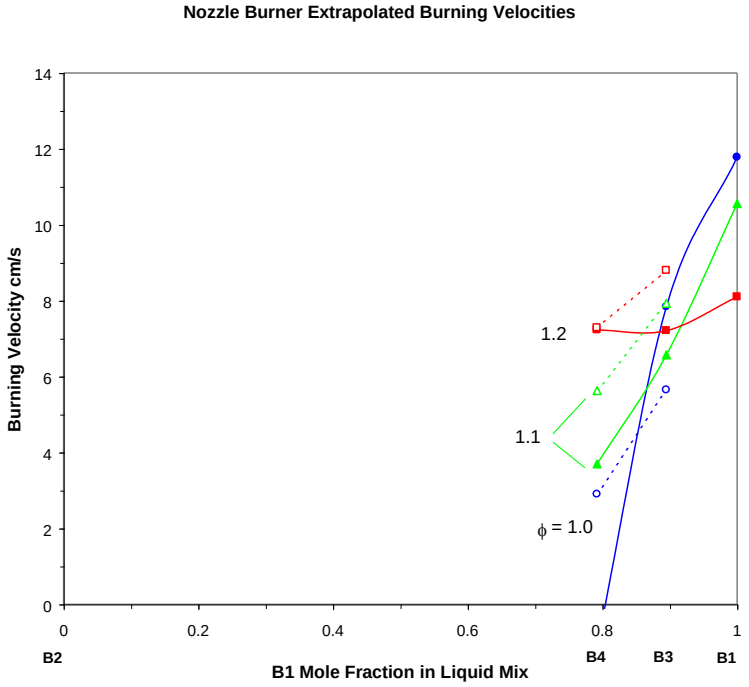

Fig. 19. Extrapolated burning velocities obtained from nozzle burner measurements of B3, B4, and B1 for ϕ=1.0, 1.1, and 1.2 with dry air (solid lines) and moist air (dotted lines, no B1 data). The data are plotted as a function of the mole fraction of B1 in the liquid fuel. Uncertainty in the estimates is about $\pm$ 1.3 cm/s for all data points.

The data of Fig. 19 are re-plotted in Fig. 20, in which the extrapolated burning velocity is shown as a function of the equivalence ratio ϕ for each fuel. As described above, use of moist air decreases the variation with ϕ for B4, switches the dependence for B3 (although neither wet or dry air has a strong ϕ dependence). B1 flames appear to have their peak burning velocity at ϕ=1.0, whereas, increasing B2 content shifts the flames to a peak burning velocity at richer conditions.

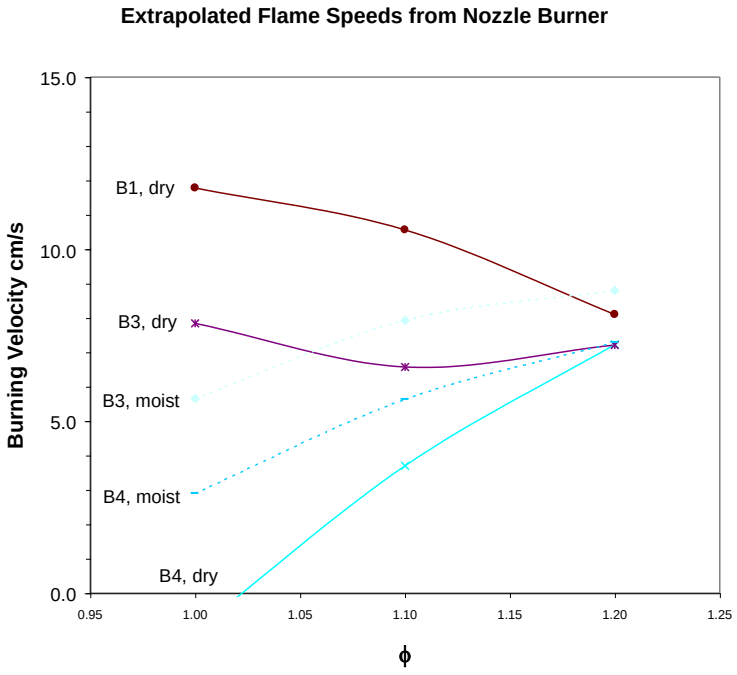

Fig. 20. Extrapolated burning velocities obtained from nozzle burner measurements of B3, B4, and B1 for ϕ=1.0, 1.1, and 1.2 with dry air (solid lines) and moist air (dotted lines, no B1 data). The data are plotted as a function of the mole fraction of B1 in the liquid fuel. Uncertainty in the estimates is about ± 1.3 cm/s for all data points.

Based on what we know about the high-temperature reaction of mixtures containing hydrocarbons and halogens [5, 10-15] it is possible to speculate about the reasons for the behavior shown in Fig. 19. Because it contains a high fraction of a non-reactive halogen, B2 acts much like a fire suppressant, trapping the reactive hydrogen radicals in the main reaction zone of the flame. Since rich flames typically have higher mole fractions of H-atom in the reaction zone, they will be less sensitive to the amount of B2 in the mixture, until higher mole fractions of B2 are added. With added water vapor the effect is similar: the water increases H atom mole fraction in the reaction zone, making the flames less sensitive to the amount of B2 (in the range plotted here). As more B2 is added, the curves should again drop off steeply. It should be cautioned that the curves in Figs. 4 to 15 are likely to be non-linear, so that the actual burning velocities may drop off more rapidly as the proportion of CH_4 in the fuel stream is reduced. This effect is probably not pertinent for pure B1 (which itself has unity hydrogen to halogen ratio) but will likely be true for flames with increasing B2 content. Thus, the estimates of the burning velocities from the extrapolations are likely to be upper limits.

5. Conclusions

The data in Fig. 19 for the nozzle burner extrapolations are summarized in Table 1 below. Also listed are results for B4 obtained by varying the value of $X_{O2,ox}$ in the nozzle burner with moist air at ϕ=1.0, and data for B3 and B4 at ϕ=1.0 with dry air from the Powling burner. The listed uncertainties for the extrapolations are based upon the average of the absolute uncertainties from the measurements for that fuel and ϕ, at lower values of X where data were collected.

Table 1. Estimated burning velocities of flames of B4, B3, and B1 for ϕ=1.0, 1.1, and 1.2 with moist and dry air obtained from the nozzle and Powling burners measurement.

Agent	S_L from extrapolation cm/s, ϕ = 1.0	ϕ = 1.1	ϕ = 1.2
Nozzle Burner, Dry Air, vary Xbi			
B4	0.0 ± 1.3	3.7 ± 1.4	7.2 ± 1.6
B3	7.8 ± 1.3	6.6 ± 1.2	7.2 ± 1.5
B1	11.8 ± 1.5	10.6 ± 1.2	8.1 ± 1.0
Nozzle Burner, Moist Air, vary Xbi			
B4	2.9 ± 1.1	5.6 ± 1.1	7.3 ± 1.2
B3	5.7 ± 1.2	7.9 ± 1.1	8.8 ± 0.8
Nozzle Burner, Moist Air, vary $X_{O2,ox}$			
B4	4.3 ± 1.7		
Powling Burner, Dry			
B4*	<6.4 ± 1.0		
B3**	<4 ± 1.0		

* 200 °C preheat, and flame area not measured.
** tests conducted in a highly transient way.

As described above, the estimated burning velocity for B4 with moist air from extrapolations with varying oxygen mole fraction (4 cm/s) and from extrapolations with varying fraction of B4 vs. methane in the fuel (3 cm/s) are consistent with each other. The Powling burner was only operated with B4 and dry air, and here the estimated burning velocity (<6.4 cm/s) is somewhat higher than the values from the nozzle burner (0 cm/s). The Powling burner was at about 200 °C preheat, however, and the flame size was not measured; inclusion of both of these effects would lower the estimated burning velocity by more than a factor of two. For B3 in the Powling burner with dry air, because of the way the data were collected (under highly transient conditions since steady operation was not possible) there is too much scatter in the data at this point for the data to be useful for comparison with the nozzle burner extrapolations.

For the agents C1 and C2, the nozzle burner proved to be a very effective method for determining the flame speeds, and the estimated peak burning velocities are 29.3 cm/s and 73.5 cm/s. For C2, the flame tip at the highest burning velocities started to wrinkle slightly, and this phenomenon may have increased the apparent burning velocity; under truly laminar conditions (if they are achievable) the burning velocity may be slightly lower.

Based on the present results, it is possible to make recommendations for any future determinations of the flame speeds of these compounds. Since flames of some of the compounds (particularly those richer in B2) are hydrogen deficient, tests should be conducted with known and constant values of added water vapor, preferably moist air at relative humidity of 50% or greater. These tests will provide the highest values of the flame speeds for these compounds.

The nozzle burner works well but typically can only get to 60 % or 80 % of B1, B3 or B4 (i.e., still 20 % to 30 % CH_4) as the fuel, and hence requires significant extrapolation to deduce the values for pure B3 or B4. Tests with varying oxygen mole fraction and pure B3 and B4 might prove useful, especially since richer flames (not yet tested by this technique) will be more stable and will require less of an extrapolation.

Detailed chemical kinetic modeling of the flames' structure would clearly provide insight into the behavior of these compounds in the present burners. Validation of the model under conditions where tests are possible would provide confidence that the models can be used to give much better extrapolation to regions not experimentally accessible. We have performed preliminary calculations for C1 and C2 but further work is necessary before the results can be used. The NIST chemical kinetic mechanism was developed to study the *inhibition* of hydrocarbon flames by HFCs, as opposed to combustion of the pure compounds. For the intended application, many assumptions were made in the model development. In using the mechanism for C1 and C2 combustion, some of those assumptions would need to be re-evaluated. Nonetheless, as-is, the mechanism (based on about 125 species and 1000 elementary reactions) predicted the burning velocity of C2 flames within 20 % of the measured value, but the predictions of the burning velocity of C1 flames is low by about a factor of three.

For tests of pure B1-B4 with moist air, the Powling burner, in its standard configuration, appears to be of limited use. It was not possible to stabilize flames of B4 and with dry air without added methane; however, with moist air and at richer conditions, it may be possible to get stable flames. Nonetheless, some correction for the large preheat is still necessary since this condition can change the burning velocity by a factor of two. Flames of B1 and B3, with or without added water vapor, are too fast and quickly become cellular so that measurements of flat, laminar flames in this burner do not appear possible. Flames of B2 appear to be too weak to stabilize. It may be possible with all agents to use mixtures of inert or reactive additives to obtain data and then extrapolate into regions of interest; however, some way to treat the high degree of preheat in this burner will still be necessary.

It should be possible to construct a hybrid burner consisting of a water-cooled sintered metal burner, similar to that used by Botha and Spalding [16] with the stabilizing screen and honeycomb matrix of Powling. We constructed such a burner but did not have time to optimize its performance and properly assess whether it will overcome the problems with overheating and cellular flame structure. Other techniques are available, including the twin, premixed, counterflow method [17], but these approaches are of somewhat greater complexity because of the need for laser-Doppler velocimetry measurements for accurate flame speed determinations.

References

[1] Powling J (1949) A new burner method for the determination of low burning velocities and limits of inflammability. *Fuel* 28(2):25-28.

[2] Egerton AC , Thabet SK (1952) Flame propagation: the measurement of burning velocities of slow flames and the determination of limits of combustion. *Proceedings of the Royal Society (London) Series A-Mathematical and Physical Sciences* 211:455-471.

[3] Badami GN , Egerton AC (1955) The determination of burning velocities of slow flames. *Proceedings of the Royal Society of London Series A Mathematical and Physical Sciences* 228(1174):297-322.

[4] Mache H , Hebra A (1941) *SitzungsberÖsterreichAkadWiss* IIa, 150:157.

[5] Linteris GT , Truett L (1996) Inhibition of premixed methane-air flames by fluoromethanes. *Combust Flame* 105(1-2):15-27. https://doi.org/Doi 10.1016/0010-2180(95)00152-2

[6] Rumminger MD , Linteris GT (2000) Inhibition of premixed carbon monoxide-hydrogen-oxygen-nitrogen flames by iron pentacarbonyl. *Combust Flame* 120(4):451-464. https://doi.org/Doi 10.1016/S0010-2180(99)00114-5

[7] Van Wonterghem J , Van Tiggelen A (1954) L'epaisseur et la vitesse de propagation du front de flamme. *B Soc Chim Belg* 63:235-260.

[8] Andrews GE , Bradley D (1972) Determination of burning velocities: a critical review. *Combust Flame* 18(1):133-153. https://doi.org/10.1016/s0010-2180(72)80234-7

[9] UTHSCA (1996) ImageTool, V2.00, Image Tool is a free Windows95-based program developed at the University of Texas Health Science Center at San Antonio, Texas and available from the Internet by anonymous FTP from ftp://maxrad6.uthscsa.edu or http://ddsdx.uthscsa.edu

[10] Linteris GT, Burgess DR, Babushok V, Zachariah M, Tsang W, Westmoreland P (1998) Inhibition of premixed methane-air flames by fluoroethanes and fluoropropanes. *Combust Flame* 113(1-2):164-180.

[11] Linteris GT , Gmurczyk GW (1995) Prediction of HF formation during suppression. *Fire suppression system performance of alternative agents in aircraft engine and dry bay laboratory simulations*, ed R.G.Gann (National Institute of Standards and Technology, Gaithersburg, MD), pp 201-318.

[12] Fallon GS, Chelliah HK, Linteris GT (1996) Chemical effects of CF_3H in extinguishing counterflow CO/Air/H_2 diffusion flames. *Proc Combust Inst* 26(0):1395-1403.

[13] Linteris GT (1996) Numerically Predicted Structure and Burning Velocity of Premixed CO-Ar-O_2-H_2 Flames Inhibited by CF_3H. *Combust Flame* 107(1-2):72-84.

[14] Burgess Jr DR, Zachariah MR, Tsang W, Westmoreland PR (1995) Thermochemical and chemical kinetic data for fluorinated hydrocarbons. *Prog Energy Combust Sci* 21(6):453-529. https://doi.org/10.1016/0360-1285(95)00009-7

[15] Linteris GT (1995) Effect of inhibitor concentration on the inhibition mechanism of fluoromethanes in premixed methane-air flames. *Halon replacements: Technology and Science, ACS Symposium Series 611*, eds Miziolek AW & Tsang W (American Chemical Society, Washington, D.C.), pp 260-274.

[16] Botha J , Spalding DB (1954) The laminar flame speed of propane/air mixtures with heat extraction from the flame. *Proceedings of the Royal Society of London Series A Mathematical and Physical Sciences* 225(1160):71-96.

[17] Vagelopoulos CM , Egolfopoulos FN (1994) Laminar Flame Speeds and Extinction Strain Rates of Mixtures of Carbon Monoxide with Hydrogen, Methane, and Air. *Proc Combust Inst* 25:1317-1323.